Support Information

Efficient charge transport via limited π–π interactions between naphthyl carbon atoms in a metal-organic framework

Yong Yan,[a,b] Zhen-Yu Li,[c] Harald Krautscheid[b,*] and Ning-Ning Zhang[a,*]

[a] School of Chemistry and Chemical Engineering, Liaocheng University, Liaocheng 252059, China.
E-mail: zhangningning@lcu.edu.cn

[b] Fakultät für Chemie und Mineralogie, Institut für Anorganische Chemie, Universität Leipzig, Johannisallee 29, 04103 Leipzig, Germany
E-mail: Krautscheid@rz.uni-leipzig.de

[c] School of Environmental and Material Engineering, Yantai University, Yantai 264005, China.

1. Experimental section

1.1. Materials and measurements. All reagents and chemicals were commercially purchased and used directly without further purification. The organic ligand 2,7-dihydroxybenzo[*lmn*][3,8]phenanthroline-1,3,6,8(2*H*,7*H*)-tetraone (H_2ONDI) was successfully synthesized by following reported method.[1] Element analysis was performed on an elementar vario EL cube microanalyzer. Thermogravimetric (TG) analyses were recorded in Al_2O_3 crucibles on a STA449F5-QMS403D simultaneous thermal analyzer with Al_2O_3 crucibles under N_2 (20 mL·min^{-1}) at a heating rate of 10 K·min^{-1} over the scope 30−800 °C. Powder X-ray diffraction (PXRD) patterns were collected on a SmartLab 9 Kw diffractometer using Cu K_α radiation (λ = 1.5406 Å, 450 W) at room temperature. UV-Vis absorption spectra were collected on UH4150 UV-Vis-NIR spectrophotometer with an integrating sphere attachment and pure $BaSO_4$ as the baseline. Electron spin resonance (ESR) spectra were performed on an EPR-200Plus electron paramagnetic resonance spectrometer (Chinainstru & Quantumtech (Hefei) Co., Ltd.) at X-band frequency (100 KHz).

1.1.1. Synthesis of single crystals of ***1***: A mixture of $Cd(NO_3)_2·4H_2O$ (15 mg, 0.5 mmol) and H_2ONDI (15 mg, 0.05 mmol) was suspended in a mixed solution of 2 mL DMF and 2 mL CH_3CN. The suspension was sealed in a Teflon-lined autoclave and heated at 120 °C for 72 hours, then allowed to cool to room temperature at a rate of 10 °C/h. Brown crystals were obtained from the product mixture. Due to the presence of some impurities, this product cannot be used for further characterization.

1.1.2. Synthesis of microcrystalline ***1***: A mixture of CdI_2 (18 mg, 0.05 mmol) and H_2ONDI (15 mg, 0.05mmol) was suspended into a mixed solvent containing 3 mL DMF and 1.5 mL CH_3CN. After sealing the mixture in a Teflon lined autoclave, it was kept at 120 °C for 72 h, and then was allowed to cool down to 30 °C at a rate of 10 °C/h. Brown crystalline products filtered and washed with DMF and EtOH several times. After drying, the product weight is approximately 14 mg with a yield of 65 %. Anal. Calc. (%) for $\{[Cd(C_{14}H_4N_2O_6)]·0.25\ DMF\}_n$ (M = 426.65 g/mol): C, 41.48; H, 1.35; N, 7.38. Found (%): C, 41.77; H, 1.59; N, 7.65. The disordered guest molecules were further validated by TG analysis. The variation in reaction conditions between the microcrystalline powder and single crystal synthesis resulted in different amounts of disordered solvents in the pores.

2.2. X-ray crystallography

Single-crystal X-ray diffraction measurements of compound **1** was carried out on a STOE STADIVARI equipped with an X-ray micro-source (Cu-Kα, λ = 154.186 pm) and a DECTRIS Pilatus 300k detector. Their crystal structures were solved through direct methods and refined using SHELX.[2] The hydrogen atoms of the ligands were added geometrically and treated using the riding model. The final structures were refined using a full-matrix least-squares refinement on F^2. All calculations were performed using the Olex2 crystallographic software.[3] Crystallographic data of compound **1** was summarized in **Table S1**. The crystal structure of compound **1** was previously published as a CSD Communication article by one of our co-authors: Yong Yan CCDC 2383757: Experimental Crystal Structure Determination, 2024, DOI: 10.5517/ccdc.csd.cc2l0hdj.

2.3. Electrical conductivity measurements

Crystalline powders of **1** were pressed into square pellets with a size of 5×5×0.39 mm. respectively. The conductivities were measured using a Keithley 2450 sourcemeter in a nitrogen atmosphere by employing the two-contact method. Viscous Ag paste was applied to two sides of a square, pellet and extended onto a Cu film. Tungsten steel probes were then brought into contact with the Ag paste on the Cu film surface to complete the electrical circuit.[4]

The specific electrical conductivity σ was calculated by following the formula of $\sigma = \frac{I}{V} \cdot \frac{l}{l \cdot t}$, where l is the length of the square plate, t represents the thickness of the pressed pellets. The activation energy was estimated according to the Arrhenius equation $\sigma = \sigma_0 \cdot e^{-\frac{E_a}{K_B T}}$ (K_B is the Boltzmann constant and T represents the absolute temperature).

2.4. Solid-state cyclic voltammetry (CV) measurements

Approximately 6 mg compound **1** was milled several times and then 0.5 mL of ethanol, 0.5 mL of DMF, and 20 μL of a 5% w/w Nafion solution were added in sequence. The mixture was further ground and ultralsonicated. Appropriately 40 μL of the well-dispersed mixture was drop-cast onto the precleaned glassy carbon electrode and dried in air. A Pt wire and an Ag^+/Ag electrode acted as the counter and the reference electrodes, respectively. Electrochemical measurements were carried out in 0.1 M $[(n\text{-}Bu)_4N]PF_6$ acetonitrile solution

bubbled with N_2. The reduction potentials of **1** was obtained from the cyclic voltammogram and referenced with Fc/Fc^+ as the internal standard.

2.5. Computational details

2.5.1. Calculation of intermolecular interactions of compound **1**. The plots of the electron density (ρ) and reduced density gradient ($s = 1/(2(3\pi^2)^{1/3})|\nabla\rho|/\rho^{4/3}$) were obtained by density functional theory calculations.[5] Calculations were performed with the B3LYP functional and the 6-311G (d,p) basis set,[6] using the Gaussian 16 program.[7] The results were analyzed by Multiwfn.[8]

2.5.2. Calculation of theoretical optical absorption spectrum. The mode of π–dimer was directly built from crystal structure data of **1**. The LC-PBE functional[9] and the 6-311g(d,p) basis set[6] were employed to conduct calculation. The results were analyzed by Multiwfn.[8]

2.5.3. The band structure and DOS were calculated using the CASTEP package.[10] The structural model of **1** was built directly from the single-crystal X-ray diffraction data. The exchange-correlation energy was described by the PBE functional within the GGA.[11] The norm conserving pseudopotentials[12] were chosen to modulate the electron−ion interaction for **1**. The plane-wave cutoff energy was set as 750 eV. The Fermi level is set by default to the energy level of the valence band maximum (VBM). Other parameters were set to default values.

2. Table section

Table S1 The crystal data and structure refinement for compound **1**.

Items	Compound **1**[#]
Empirical formula	$CdC_{14}H_4N_2O_6$*
Formula weight/g·mol^{-1}	408.59*
Temperature/K	180
Crystal system	monoclinic
Space group	*C*2/c
a, Å	21.5322(9)
b, Å	9.4140(3)
c, Å	7.3067(3)
α (deg)	90
β (deg)	90.868(3)
γ (deg)	90
V/Å^3	1480.9(1)
Z	4
λ/Å	1.54186
D_{calc}(g cm-3)	1.833*
μ/mm^{-1}	12.136*
F(000)	792*
Reflections collected	6816
Independent reflections	1382(R_{int} = 0.0549)
Observed refl. [I > 2σ(I)]	1269
Completeness	0.969 (θ = 70.557)
GOF	1.015
R_1[a], wR_2[b] [I > 2σ(I)]	0.0268, 0.0669
R_1[a], wR_2[b] (all data)	0.0293, 0.0678
a) $R1 = \Sigma\|\|F_o\|-\|F_c\|\| / \Sigma\|F_o\|$; b) $wR_2 = [\Sigma w(F_o^2-F_c^2)^2 / \Sigma w(F_o^2)^2]^{1/2}$	
* The PLATON mask has been applied in the Olex2. Formula and numbers for formula weight, calculated density, absorption coefficient and F(000) correspond to the atoms included in the refinement. The disordered solvents and counter ions have not been included into the sum formula. A solvent mask was calculated and 98 electrons were found in a volume of 324 A^3 in 1 void per unit cell. This is consistent with the presence of 0.6 [DMF] per formula unit which account for 96 electrons per unit cell. The variation in reaction conditions between the microcrystalline powder and single crystal synthesis resulted in different amounts of disordered solvents in the pores.	
# The crystal structure of compound **1** was previously published as a CSD Communication article by one of our co-authors: Yong Yan CCDC 2383757:	

Experimental Crystal Structure Determination, 2024, DOI: 10.5517/ccdc.csd.cc2l0hdj.

Table S2 A comparative table of the electrical conductivities of semiconductive coordination polymers featuring naphthalenediimides (NDI).

NDI-derived Compounds	**Electrical conductivity**	**Reference**
ZnNDI-A ZnNDI-B ZnNDI-C	2×10^{-7} S/cm (Pellets) 1×10^{-9} S/cm (Pellets) 3×10^{-10} S/cm (Pellets)	*Chem. Sci.,* **2020**, *11*, 1342–1346
PMC-1	4.5×10^{-6} S/cm (Pellet)	*J. Am. Chem. Soc.*, **2019**, *141*, 6802–6806.
PMC-2	1.4×10^{-6} S/cm (single crystals)	*Chem. Commun.*, **2020**, *56*, 8619–8622.
K-ONDI-140 K-ONDI-150 K-ONDI-160	1.0×10^{-7} S/cm (Pellets) 4.3×10^{-7} S/cm (Pellets) 6.5×10^{-6} S/cm (Pellets)	*Inorg. Chem. Front.,* **2022**, *9*, 5016–5023.
La-ONDI-DMA La-ONDI-DMF La-ONDI-Catechol	2.1×10^{-8} S/cm (Pellets) 2.4×10^{-6} S/cm (Pellets) 5.9×10^{-6} S/cm (Pellets)	*Dalton Trans.,* **2022**, *51*, 15946–15953.
Mn-ONDI-1 CdCl-ONDI	3.7×10^{-8} S/cm (Pellets) 3.5×10^{-9} S/cm (Pellets)	*Dalton Trans*., **2022**, *51*, 12709–12716
Ca-ONDI Sr-ONDI	1.03×10^{-7} S/cm (Pellets) 2.21×10^{-7} S/cm (Pellets)	*Chem. Commun*., **2021**, *57*, 10407–10410.
Co-pyNDI Ni-pyNDI Zn-pyNDI	8.79×10^{-8} S/cm (Pellets) 6.03×10^{-8} S/cm (Pellets) 8.48×10^{-11} S/cm (Pellets)	*Angew. Chem. Int. Ed.,* **2023**, *62*, e202215.
$\{[BaMn(ONDI)(H_2O)_3]\cdot H_2O\}_n$	1.5×10^{-8} S/cm (Pellets)	*Chem. Eng. J.*, **2024**, 491, 152054.
$[K(HONDI)(H_2O)_2]_n$ (1) $[K(HONDI)]_n$ (2)	2.3×10^{-6} S/cm (Pellets) 1.9×10^{-7} S/cm (Pellets)	*Inorg. Chem.*, **2024**, 63, 15485–15492.
$\{[Cd(ONDI)]\cdot x$ DMF$\}_n$	**3.1×10^{-7} S/cm (Pellets)**	**This work**

3. Figure section

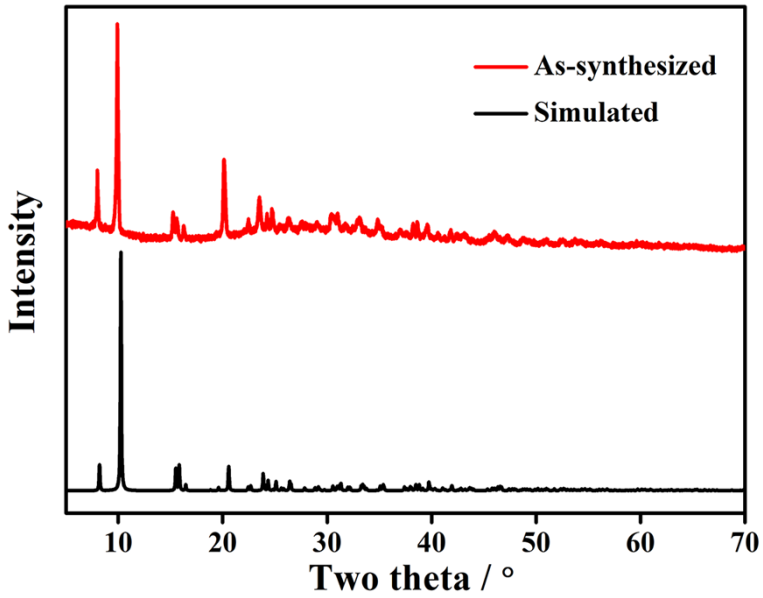

Fig. S1 The experimental and simulated PXRD patterns of compound **1**.

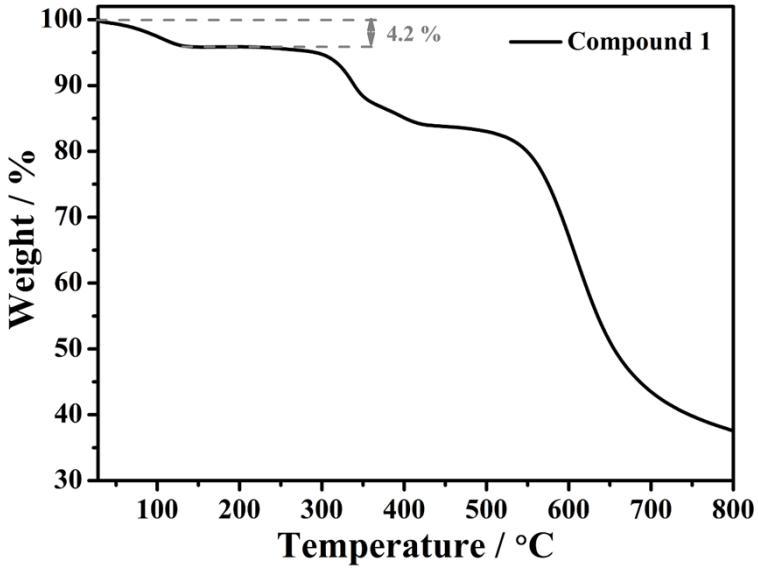

Fig. S2 The TG curve of compound **1**. The weight loss of 4.2 % below 200 °C is assigned to the loss of disordered guest solvent DMF (calculated value: 4.3 %).

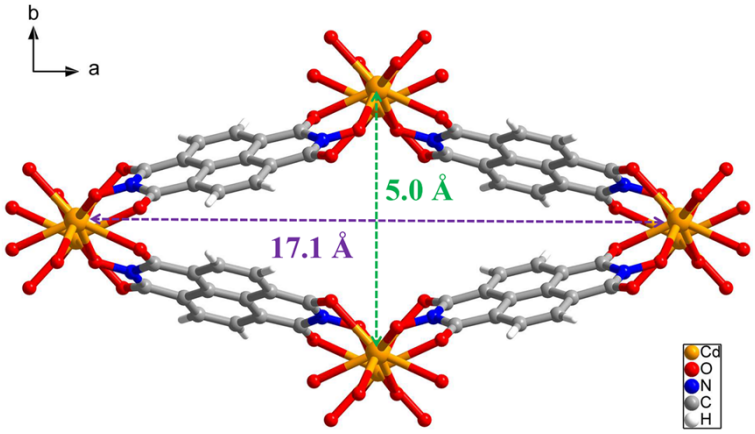

Fig. S3 The aperture size of channels along the *c* axis in compound **1**. The aperture size was estimated by measuring the distances between symmetric cadmium atoms and subtracting their van der Waals radius.

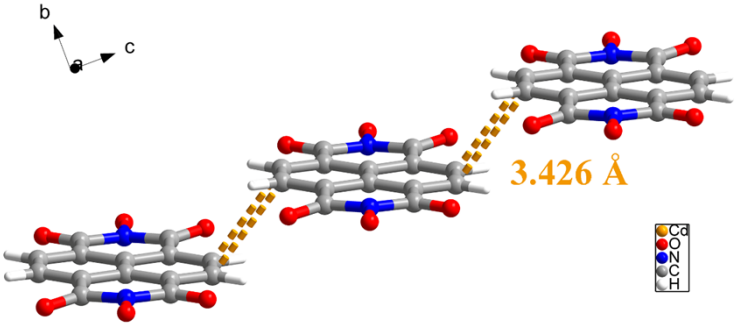

Fig. S4 Assembly of $ONDI^{2-}$ ligands viewed along the *a* axis. This view shows that there is no intermolecular overlap region between the adjacent ligands.

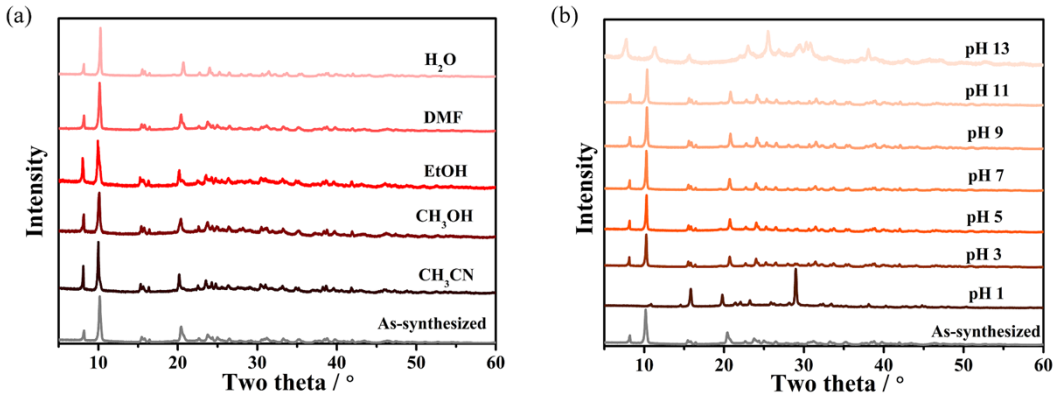

Fig. S5 The PXRD patterns of compound **1** after immersion in various solvents (a) and exposure to different pH conditions (b) for three days.

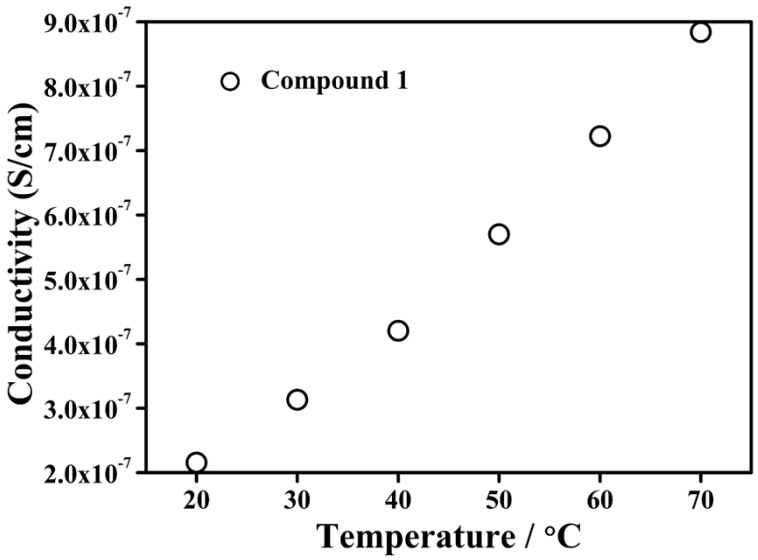

Fig. S6 Temperature-dependent conductivity plot of compound **1**.

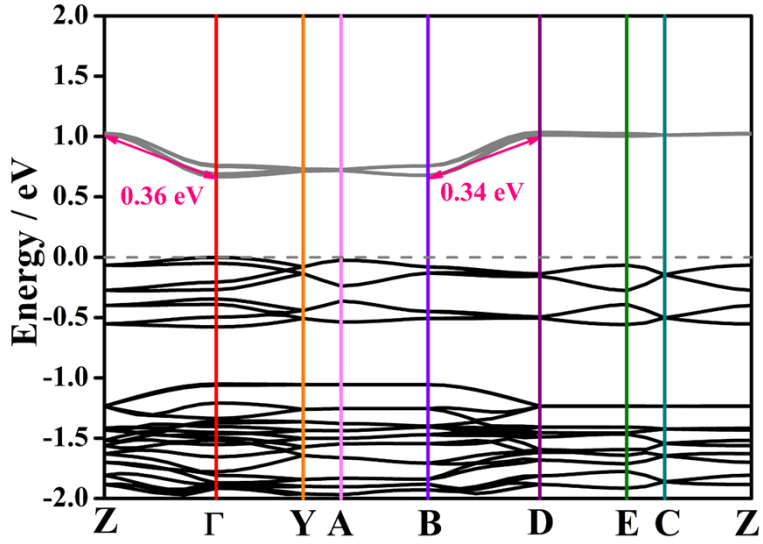

Figure S7. Detailed dispersion widths of valence band line closest to the Fermi level in compound **1**.

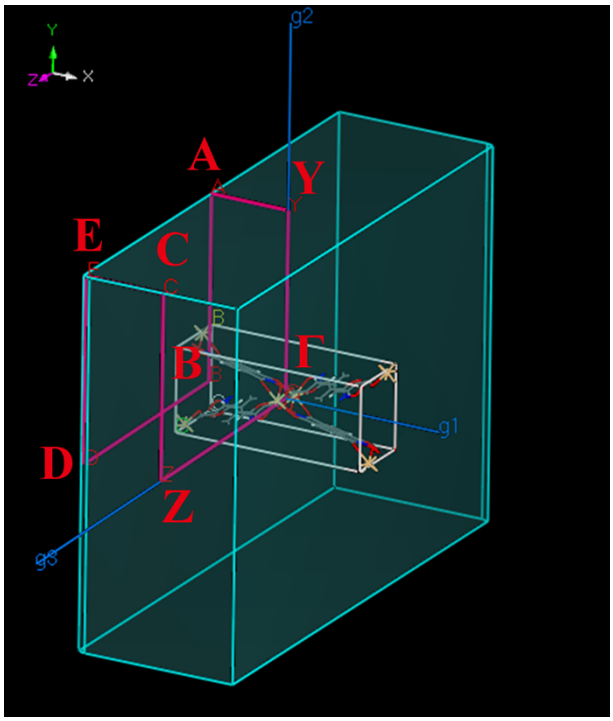

Figure S8. The K-point path in Brillouin zone of **1**.

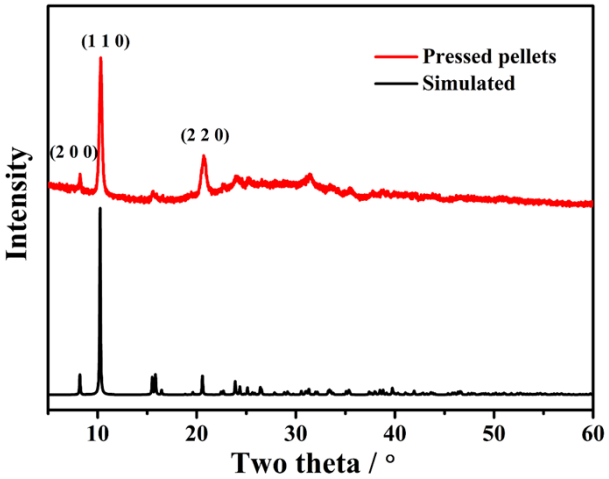

Figure S9 The PXRD patterns of pressed pellets of compound **1**. The ideal plane (-5 0 112), which is perpendicular to the c-axis, does not show any distinct peaks.

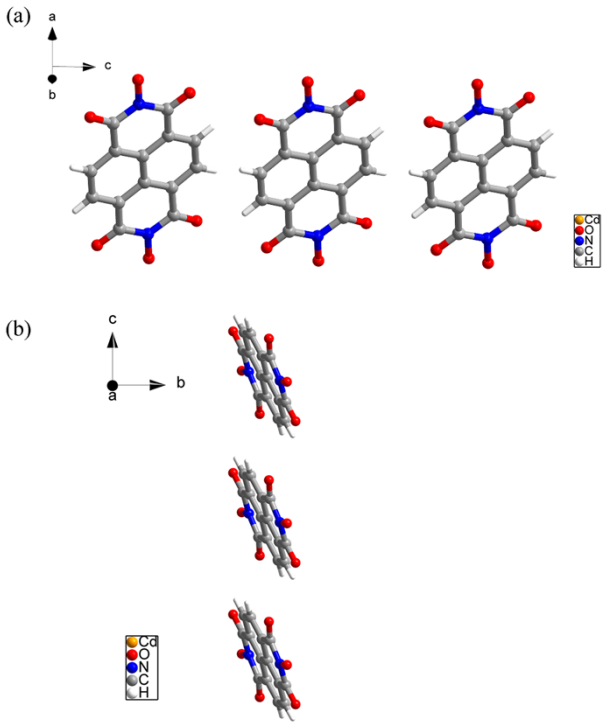

Figure S10 Views of ligands column toward the (1 1 0) plane (a) and (2 0 0) plane (b) in compound **1**.

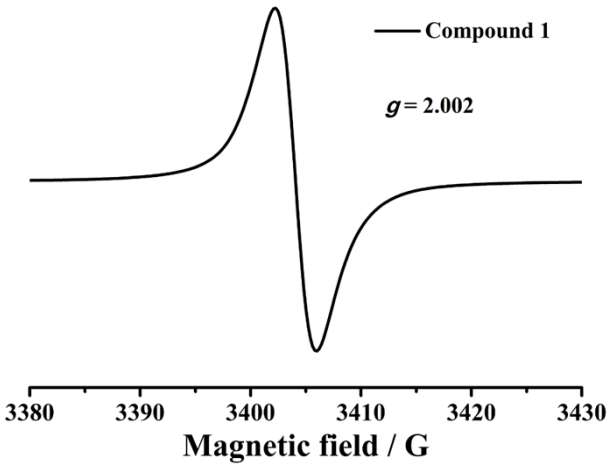

Fig. S11 The solid-state electron paramagnetic resonance (EPR) spectrum of compound **1** (5 mg).

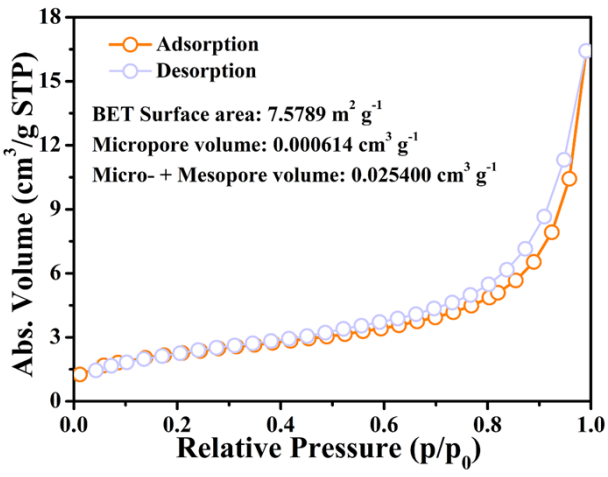

Fig. S12 N_2 adsorption and desorption isotherm of compound **1** at 77 K. The result show that compound **1** is nearly non-porous to N_2, possibly due to the presence of residual DMF molecules within the channels, which obstruct N_2 from reaching the pores (DMF size: 4.018 × 5.943 × 6.864 Å vs. aperture size: 17.1 × 5.0 Å). Freshly prepared Compound **1** was exchanged with fresh MeOH six times over two days, followed by evacuation at 100 °C under vacuum for 8 hours. N_2 adsorption measurements were conducted on an ASAP 2460 at 77 K.

4. References

1. D. Liu, Y. Lu, Y. J. Lin, G. X. Jin, Donor−acceptor [2]- and [3] catenanes assembled from versatile pre-organized Cp*Rh/Ir directed pseudorotaxane tectons. *Chem. - Eur. J.*, 2019, 25, 14785−14789.

2. G. M. Sheldrick, A short history of SHELX, *Acta Crystallogr., Sect. A: Found. Crystallogr.*, 2008, 64, 112–122.

3. O. V. Dolomanov, L. J. Bourhis, R. J. Gildea, J. A. K. Howard, H. Puschmann, OLEX2: A complete structure solution, Refinement and analysis program, *J. Appl. Cryst.* 2009, 42, 339–341.

4. N.-N. Zhang, Y. Yan, Z.-Y. Li, H. Krautscheid, Semiconductive potassium hydroxamate coordination polymers with dual charge transport paths originating from the π−π stacking columns, *Inorg. Chem.*, 2024, 63, 15485−15492

5. E. R. Johnson, S. Keinan, P. Mori-Sánchez, J. Contreras-García, A. J. Cohen, W. Yang, Revealing noncovalent interactions, *J. Am. Chem. Soc.*, 2010, 132, 6498–6506.

6. C. T. Lee, W. T. Yang, R. G. Parr, Development of the colle-salvetti correlation-energy formula into a functional of the electron density, *Phys. Rev. B.*, 1988, 37, 785–789.

7. Gaussian 16, Revision C.01, M. J. Frisch, G. W. Trucks, H. B. Schlegel, G. E. Scuseria, M. A. Robb, J. R. Cheeseman, G. Scalmani, V. Barone, G. A. Petersson, H. Nakatsuji, X. Li, M. Caricato, A. V. Marenich, J. Bloino, B. G. Janesko, R. Gomperts, B. Mennucci, H. P. Hratchian, J. V. Ortiz, A. F. Izmaylov, J. L. Sonnenberg, D. Williams-Young, F. Ding, F. Lipparini, F. Egidi, J. Goings, B. Peng, A. Petrone, T. Henderson, D. Ranasinghe, V. G. Zakrzewski, J. Gao, N. Rega G. Zheng, W. Liang, M. Hada, M. Ehara, K. Toyota, R. Fukuda, J. Hasegawa, M. Ishida, T. Nakajima, Y. Honda, O. Kitao, H. Nakai, T. Vreven, K. Throssell, J. A. Montgomery, Jr., J. E. Peralta, F. Ogliaro, M. J. Bearpark, J. J. Heyd, E. N. Brothers, K. N. Kudin, V. N. Staroverov, T. A. Keith, R. Kobayashi, J. Normand, K. Raghavachari, A. P. Rendell, J. C. Burant, S. S. Iyengar, J. Tomasi, M. Cossi, J. M. Millam, M. Klene, C. Adamo, R. Cammi, J. W. Ochterski, R. L. Martin, K. Morokuma, O. Farkas, J. B. Foresman, and D. J. Fox, Gaussian, Inc., Wallingford CT, 2016.

8. T. Lu, F. W. Chen, Multiwfn: A multifunctional wavefunction analyzer, *J. Comput. Chem.,* 2012, *33*, 580−592.

9. M. Seth, T. Ziegler, Range-separated exchange Functionals with slater-type functions, *J. Chem. Theory Comput.*, 2012, 8, 901−907.

10. S. J. Clark, M. D. Segall, C. J. Pickard, P. J. Hasnip, M. I. J. Probert, K. Refson, M. C. Payne, First

principles methods using CASTEP, *Z. Kristallogr. - Cryst. Mater.*, 2005, 220, 567−570.

11. B. Hammer, L. B. Hansen, J. K. Norskov, Improved adsorption energetics within density-functional theory using revised perdew-burke-ernzerhof functionals, *Phys. Rev. B: Condens. Matter Mater. Phys.*, 1999, 59, 7413−7421.

12. J. S. Lin, A. Qteish, M. C. Payne, V. Heine, Optimized and transferable nonlocal separable ab initio pseudopotentials, *Phys. Rev. B: Condens. Matter Mater. Phys*., 1993, 47, 4174−4180.